

## Josephson supercurrent in Nb/InN-nanowire/Nb junctions

R. Frielinghaus, I. E. Batov, M. Weides, H. Kohlstedt, R. Calarco, and Th. Schäpers

Citation: *Appl. Phys. Lett.* **96**, 132504 (2010);

View online: <https://doi.org/10.1063/1.3377897>

View Table of Contents: <http://aip.scitation.org/toc/apl/96/13>

Published by the [American Institute of Physics](#)

---

### Articles you may be interested in

[Supercurrent in Nb/InAs-nanowire/Nb Josephson junctions](#)

*Journal of Applied Physics* **112**, 034316 (2012); 10.1063/1.4745024

[Ballistic one-dimensional transport in InAs nanowires monolithically integrated on silicon](#)

*Applied Physics Letters* **110**, 083105 (2017); 10.1063/1.4977031

[Hybrid superconductor-quantum point contact devices using InSb nanowires](#)

*Applied Physics Letters* **109**, 233502 (2016); 10.1063/1.4971394

[Electronic transport through Al/InN nanowire/Al junctions](#)

*Applied Physics Letters* **108**, 063104 (2016); 10.1063/1.4941733

[Josephson coupling across a long single-crystalline Cu nanowire](#)

*Applied Physics Letters* **110**, 222605 (2017); 10.1063/1.4984605

[Magne-to-transport analysis of an ultra-low-density two-dimensional hole gas in an undoped strained Ge/SiGe heterostructure](#)

*Applied Physics Letters* **108**, 233504 (2016); 10.1063/1.4953399

---

# Scilight

Sharp, quick summaries illuminating  
the latest physics research

Sign up for **FREE!**

AIP  
Publishing

# Josephson supercurrent in Nb/InN-nanowire/Nb junctions

R. Frielinghaus,<sup>1</sup> I. E. Batov,<sup>2</sup> M. Weides,<sup>3,a)</sup> H. Kohlstedt,<sup>3,b)</sup> R. Calarco,<sup>1</sup> and Th. Schäpers<sup>1,c)</sup>

<sup>1</sup>*Institute of Bio- and Nanosystems (IBN-1) and JARA-Fundamentals of Future Information Technology, Forschungszentrum Jülich, 52425 Jülich, Germany*

<sup>2</sup>*Institute of Solid State Physics, Russian Academy of Sciences, Chernogolovka, Moscow district, Institutskaya 2, 142432 Russia*

<sup>3</sup>*Institute of Solid State Research (IFF) and JARA-Fundamentals of Future Information Technology, Forschungszentrum Jülich, 52425 Jülich, Germany*

(Received 21 November 2009; accepted 10 March 2010; published online 1 April 2010)

We experimentally studied the Josephson supercurrent in Nb/InN-nanowire/Nb junctions. Large critical currents up to  $5.7 \mu\text{A}$  have been achieved, which proves the good coupling of the nanowire to the superconductor. The effect of a magnetic field perpendicular to the plane of the Josephson junction on the critical current has been studied. The observed monotonous decrease in the critical current with magnetic field is explained by the magnetic pair-breaking effect in planar Josephson junctions of ultra-narrow width [J. C. Cuevas and F. S. Bergeret, Phys. Rev. Lett. **99**, 217002 (2007)]. © 2010 American Institute of Physics. [doi:10.1063/1.3377897]

Superconductor/normal-conductor/superconductor (SNS) junctions with a semiconductor employed as the N-weak link material offer the great advantage that here the Josephson supercurrent can be controlled by means of the field effect.<sup>1,2</sup> Gate-controlled superconductor/semiconductor hybrid devices such as superconducting field effect transistors<sup>3</sup> or split-gate structures<sup>4</sup> have been fabricated which find no counterpart in conventional SNS structures. In addition, the high carrier mobility attainable in semiconductors in combination with the phase-coherent Andreev reflection leads to unique phenomena in the magnetotransport.<sup>5–7</sup> Usually, for these devices the semiconductor is patterned by conventional lithography. As an elegant alternative one can also directly create semiconductor nanostructures, i.e., nanowires, by epitaxial growth.<sup>8</sup> By using InAs nanowires connected to superconducting electrodes tunable Josephson supercurrents, supercurrent reversal, and Kondo-enhanced Andreev tunneling have been realized.<sup>9–11</sup>

Among the various materials used for semiconductor nanowires InN is of particular interest for semiconductor/superconductor hybrid structures, since the surface accumulation layer in InN can provide a sufficiently low resistive contact to superconducting electrodes.<sup>12–14</sup> Due to almost ideal crystalline properties of InN nanowires electronic transport along the wires, contacted by normal metal electrodes, shows quantization phenomena, i.e., flux periodic magnetoconductance oscillations.<sup>15</sup> Furthermore, the carrier concentration in the surface electron gas is of the order of  $10^{13} \text{ cm}^{-2}$  and thus about a factor of 10 larger than in InAs. Consequently when combined with superconducting electrodes one can expect low resistive SNS junctions.

Here, we report on transport studies of Nb/InN-nanowire/Nb junctions. We succeeded in observing a pronounced Josephson supercurrent and a relatively large  $I_c R_N$

product of up to 0.44 mV. The latter factor, the critical current times the normal resistance, is an important figure of merit for Josephson junctions. We devoted special attention to the dependence of the critical current  $I_c$  on an external magnetic field  $B$ , where a monotonous decrease in  $I_c$  with  $B$  was found. This experimental finding is interpreted in the framework of a recent theoretical model for the proximity effect in narrow-width junctions with dimensions comparable or smaller than the magnetic length  $\xi_B = \sqrt{\Phi_0/B}$ , where  $\Phi_0 = h/2e$  is the flux quantum.<sup>16,17</sup>

The InN nanowires used for the normal conducting part of our junctions were grown without catalyst on a Si (111) substrate by plasma-assisted molecular beam epitaxy.<sup>18</sup> The wires had a typical length of  $1 \mu\text{m}$ . The nanowires were contacted by a pair of 100-nm-thick Nb electrodes. Before the Nb sputter deposition the contact area was cleaned by  $\text{Ar}^+$  milling. The superconducting transition temperature  $T_c$  of the Nb layers was 8.5 K. The InN nanowire of the first junction (sample A) had a diameter  $d=120 \text{ nm}$  and a Nb electrode separation  $L=105 \text{ nm}$  [cf. Fig. 1 (inset)], while for the second junction (sample B) the corresponding dimen-

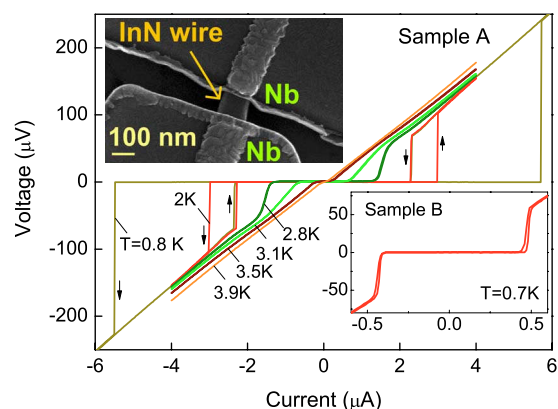


FIG. 1. (Color online)  $I$ - $V$  characteristics of sample A at various temperatures. The lower right inset shows the  $I$ - $V$  characteristics for sample B at 0.7 K. The upper left inset shows a scanning electron beam micrograph picture of sample A.

<sup>a)</sup>Present address: Physics Department University of California–Santa Barbara, 93106 Santa Barbara CA, USA.

<sup>b)</sup>Present address: Nanoelektronik, Technische Fakultät, Christian-Albrechts-Universität zu Kiel, 24143 Kiel, Germany.

<sup>c)</sup>Electronic mail: th.schaeppers@fz-juelich.de.

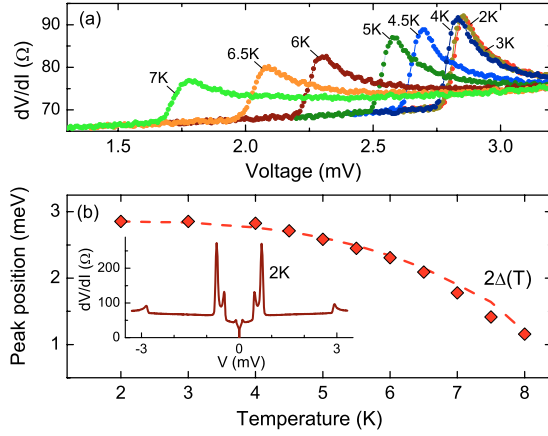


FIG. 2. (Color online) (a) Differential resistance  $dV/dI$  of sample A as a function of bias voltage at various temperatures. (b) Position of the peak assigned to  $2\Delta$  as a function of temperature. The broken line shows the expected value of  $2\Delta$  according to theory. The inset shows  $dV/dI$  at 2 K in the full bias voltage range.

sions were 85 nm and 130 nm, respectively. From measurements on back-gate transistor structures performed on nanowires prepared in the same epitaxial run a typical electron concentration of  $1 \times 10^{19} \text{ cm}^{-3}$  was determined. From measurements on nanowires contacted with normal contacts with various distances a specific resistance of  $\rho = 4.2 \times 10^{-4} \text{ } \Omega \text{ cm}$  was estimated.<sup>19</sup> Using these values we calculated a diffusion constant of  $D = 110 \text{ cm}^2/\text{s}$ .

The transport measurements were conducted in a He-3 cryostat in a temperature range from 0.7 to 10 K. The magnetic field was applied perpendicularly to the plane of the Nb electrodes. The differential resistance was measured with a lock-in amplifier by superimposing a small 17 Hz ac signal of 50 nA to the junction bias current.

The current-voltage ( $I$ - $V$ ) characteristics of sample A for various temperatures are shown in Fig. 1. As can be seen here, a clear Josephson supercurrent is observed at temperatures up to 3.5 K. At 0.8 K a critical current of  $5.7 \text{ } \mu\text{A}$  was extracted. For temperatures below 2.5 K the  $I$ - $V$  characteristics is hysteretic. The retrapping current  $I_r$ , characterized by the switching from the voltage biased state back into the superconducting state depends only slightly on temperature, with a typical value of  $2.2 \text{ } \mu\text{A}$ . As can be seen in Fig. 1 (inset), for sample B a lower critical current of  $0.44 \text{ } \mu\text{A}$  at 0.7 K was measured.

The differential resistance  $dV/dI$  as a function of the bias voltage close to  $2\Delta/e$  is shown in Fig. 2(a) for temperatures in the range from 2 to 7 K. The distinct peak and the lowering of  $dV/dI$  at its lower bias side can be attributed to the onset of multiple Andreev reflection.<sup>20,21</sup> The relatively small decrease in differential resistance at the lower bias side of the peak by about 10% compared to the higher bias side can be attributed to the presence of an interface barrier.<sup>20,21</sup> As can be seen in Fig. 2(b) (inset), more structures are found in the differential resistance by approaching zero bias. Details about these features, which we also attribute to multiple Andreev reflection, will be given in a forthcoming publication. Further evidence that the maxima shown in Fig. 2(a) can indeed be assigned to the onset of Andreev reflection at  $2\Delta/e$  is given by the plot of the peak position as a function of temperature [cf. Fig. 2(b)], since here the peak position closely follows the theoretically expected decrease of  $2\Delta$  for

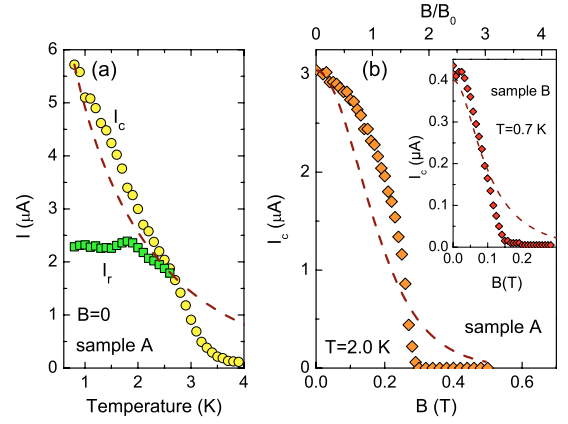


FIG. 3. (Color online) (a)  $I_c$  (○) and  $I_r$  (□) vs  $T$  of sample A. The dashed line represents the calculated values following Ref. 16. (b)  $I_c$  as a function of  $B$  of sample A. The corresponding normalized magnetic field  $B/B_0$  is given in the upper scale, with  $B_0 = \Phi_0/(Ld)$ . The dashed line represents the calculated  $I_c(B)$  dependence following Ref. 16. The inset shows the corresponding values for sample B.

an electron-phonon coupling strength of  $2\Delta_0/k_B T_c \approx 3.9$ .<sup>22</sup> Here,  $\Delta_0$  is the energy gap of the superconductor at  $T=0$ . At a temperature of 2 K and bias voltages above  $2\Delta/e$  a differential resistance of  $78 \text{ } \Omega$  is measured. If this value is taken as the normal state resistance  $R_N$  of the junction one obtains a large  $I_c R_N$  product of  $0.44 \text{ mV}$ . For sample B a normal state resistance of  $250 \text{ } \Omega$  was measured which results in a somewhat lower  $I_c R_N$  product of  $0.11 \text{ mV}$ .

As can be seen in Fig. 3(a), the critical current  $I_c$  of sample A monotonously decreases with increasing temperature. A complete suppression of the Josephson supercurrent is obtained at about 3.7 K. Up to 2 K the return current  $I_r$  is almost constant at a value of approximately  $2.3 \text{ } \mu\text{A}$ , while at higher temperatures  $T \geq 2.5 \text{ K}$   $I_r$  merges with  $I_c$ . A similar behavior of the retrapping current was observed previously in other Nb-semiconductor-Nb junctions.<sup>23</sup> As it was recently pointed out by Courtois *et al.*,<sup>24</sup> the hysteresis in the  $I$ - $V$  characteristics of proximity SNS structures can be attributed to the increase of the normal-metal electron temperature once the junction switches to the resistive state.

From the transport data of the InN nanowires one extracts an elastic mean free path of approximately 45 nm, thus the transport takes place in the diffusive regime. In addition, as stated above we have to consider the presence of an interface barrier. For this case, the critical current was studied theoretically by Hammer *et al.*<sup>16</sup> In Fig. 3(a) the corresponding theoretical curve which fits best to the experimental values is plotted. We followed the approach of Dubos *et al.*<sup>25</sup> and Carillo *et al.*<sup>26</sup> by using a reduced effective Thouless energy  $E_{Th}^*$  as a fitting parameter. The lower value of  $E_{Th}^* = 0.15 \text{ meV}$  compared to  $E_{Th} = \hbar D/L^2 = 0.67 \text{ meV}$  obtained from the transport parameters is a measure of the detrimental effect of the interface resistance.<sup>16</sup>

The magnetic field dependence of the critical current  $I_c$  of sample A is shown in Fig. 3(b). It can be seen that  $I_c$  decreases monotonously to zero, over a field scale of about 0.3 T. Note that in experiments on wider diffusive S/semiconductor/S Josephson junctions,<sup>26,27</sup>  $I_c$  exhibits standard Fraunhofer-type oscillations with the magnetic field. The absence of a magnetic interference pattern was previously observed in narrow SNS structures by Angers *et al.*<sup>28</sup> In Refs. 16 and 17 it has been shown theoretically that in

planar diffusive SNS structures the field dependence of  $I_c$  crosses over from the Fraunhofer pattern in wide junctions to a monotonic decay when the width of the normal wire is smaller than the magnetic length  $\xi_B$ . The reason for the monotonic decay of  $I_c$  is that for junctions with a width comparable or smaller than  $\xi_B$  the magnetic field acts as a pair-breaking factor. Indeed at the magnetic field  $B_0$  defined by the flux quantum through the cross section of the normal wire  $B_0 = \Phi_0 / Ld = 0.16$  T [cf. Fig. 3(b)] the magnetic length  $\xi_B$  is as large as 110 nm and thus comparable to the junction width. For sample B a similar dependence of  $I_c$  on  $B$  is observed with a full suppression of  $I_c$  at 0.2 T. By using the model of Hammer *et al.*<sup>16</sup> for the case of low transparent junctions we calculated the expected dependence of  $I_c$  on  $B$  taking the same fitting parameter:  $E_{Th}^* = 0.15$  meV, as used above. As can be seen in Fig. 3(b), a reasonable agreement between experiment and theory is obtained. The same is true for sample B with  $E_{Th}^* = 0.7$  meV [cf. Fig. 3(b), inset]. A possible reason for the discrepancy between the experimental values and theoretical curves might be that in our InN nanowires the current flows mainly in the surface accumulation layer, which leads to an inhomogeneous current distribution.

In summary, superconducting Nb/InN-nanowire/Nb junctions with large critical currents up to 5.7  $\mu$ A and large  $I_c R_N$  products up to 0.44 mV have been fabricated. Owing to the small width of nanowires a monotonous decrease in  $I_c$  with  $B$  was observed, since in this case the magnetic field is the main pair breaking factor. The present results suggest that Nb/InN-nanowire/Nb structures are well suited for fundamental research and application in nanoscaled Josephson junction-based devices.

We are grateful to A. A. Golubov (Twente University, The Netherlands) and V. V. Ryazanov (Institute of Solid State Physics RAS, Chernogolovka) for fruitful discussions and H. Kertz for support during the measurements. I.E.B. acknowledges the Russian Foundation for Basic Research, Project No. RFBR 09-02-01499 for financial support.

<sup>1</sup>A. A. Golubov, M. Y. Kupriyanov, and E. Il'ichev, *Rev. Mod. Phys.* **76**, 411 (2004).

<sup>2</sup>T. Sch apers, *Superconductor/Semiconductor Junctions*, Springer Tracts on Modern Physics Vol. 174 (Springer, Berlin, Heidelberg, 2001).

<sup>3</sup>T. Akazaki, H. Takayanagi, J. Nitta, and T. Enoki, *Appl. Phys. Lett.* **68**,

418 (1996).

<sup>4</sup>H. Takayanagi, T. Akazaki, and J. Nitta, *Phys. Rev. Lett.* **75**, 3533 (1995).

<sup>5</sup>I. E. Batov, Th. Sch apers, A. A. Golubov, and A. V. Ustinov, *J. Appl. Phys.* **96**, 3366 (2004).

<sup>6</sup>J. Eroms, D. Weiss, J. D. Boeck, G. Borghs, and U. Z ulicke, *Phys. Rev. Lett.* **95**, 107001 (2005).

<sup>7</sup>I. E. Batov, Th. Sch apers, N. M. Chitchev, H. Hardtdegen, and A. V. Ustinov, *Phys. Rev. B* **76**, 115313 (2007).

<sup>8</sup>C. Thelander, P. Agarwal, S. Brongersma, J. Eymery, L. Feiner, A. Forchel, M. Scheffler, W. Riess, B. Ohlsson, U. G osele, and L. Samuelson, *Mater. Today* **9**, 28 (2006).

<sup>9</sup>J. A. van Dam, Y. V. Nazarov, E. P. A. M. Bakkers, S. D. Franceschi, and L. P. Kouwenhoven, *Nature (London)* **442**, 667 (2006).

<sup>10</sup>Y.-J. Doh, J. A. van Dam, A. L. Roest, E. P. A. M. Bakkers, L. P. Kouwenhoven, and S. D. Franceschi, *Science* **309**, 272 (2005).

<sup>11</sup>T. Sand-Jespersen, J. Paaske, B. M. Andersen, K. Grove-Rasmussen, H. I. J rgensen, M. Aagesen, C. B. S rensen, P. E. Lindelof, K. Flensberg, and J. Nyg rd, *Phys. Rev. Lett.* **99**, 126603 (2007).

<sup>12</sup>C.-Y. Chang, G.-C. Chi, W.-M. Wang, L.-C. Chen, K.-H. Chen, F. Ren, and S. J. Pearton, *Appl. Phys. Lett.* **87**, 093112 (2005).

<sup>13</sup>F. Werner, F. Limbach, M. Carsten, C. Denker, J. Malindretos, and A. Rizzi, *Nano Lett.* **9**, 1567 (2009).

<sup>14</sup>R. Calarco and M. Marso, *Appl. Phys. A: Mater. Sci. Process.* **87**, 499 (2007).

<sup>15</sup>T. Richter, Ch. Bl omers, H. L uth, R. Calarco, M. Indlekofer, M. Marso, and Th. Sch apers, *Nano Lett.* **8**, 2834 (2008).

<sup>16</sup>J. C. Hammer, J. C. Cuevas, F. S. Bergeret, and W. Belzig, *Phys. Rev. B* **76**, 064514 (2007).

<sup>17</sup>J. C. Cuevas and F. S. Bergeret, *Phys. Rev. Lett.* **99**, 217002 (2007).

<sup>18</sup>T. Stoica, R. Meijers, R. Calarco, T. Richter, and H. L uth, *J. Cryst. Growth* **290**, 241 (2006).

<sup>19</sup>T. Richter, H. L uth, Th. Sch apers, R. Meijers, K. Jegannathan, S. E. Hernandez, R. Calarco, and M. Marso, *Nanotechnology* **20**, 405206 (2009).

<sup>20</sup>M. Octavio, M. Tinkham, G. E. Blonder, and T. M. Klapwijk, *Phys. Rev. B* **27**, 6739 (1983).

<sup>21</sup>B. A. Aminov, A. A. Golubov, and M. Yu. Kupriyanov, *Phys. Rev. B* **53**, 365 (1996).

<sup>22</sup>J. P. Carbotte, *Rev. Mod. Phys.* **62**, 1027 (1990).

<sup>23</sup>Th. Sch apers, A. Kaluza, K. Neurohr, J. Malindretos, G. Creclius, A. van der Hart, H. Hardtdegen, and H. L uth, *Appl. Phys. Lett.* **71**, 3575 (1997).

<sup>24</sup>H. Courtois, M. Meschke, J. T. Peltonen, and J. P. Pekola, *Phys. Rev. Lett.* **101**, 067002 (2008).

<sup>25</sup>P. Dubos, H. Courtois, B. Pannetier, F. K. Wilhelm, A. D. Zaikin, and G. Sch on, *Phys. Rev. B* **63**, 064502 (2001).

<sup>26</sup>F. Carillo, D. Born, V. Pellegrini, F. Tafuri, G. Biasiol, L. Sorba, and F. Beltram, *Phys. Rev. B* **78**, 052506 (2008).

<sup>27</sup>K. Neurohr, Th. Sch apers, J. Malindretos, S. Lachenmann, A. I. Braginski, H. L uth, M. Behet, G. Borghs, and A. A. Golubov, *Phys. Rev. B* **59**, 11197 (1999).

<sup>28</sup>L. Angers, F. Chiodi, G. Montambaux, M. Ferrier, S. Gu eron, H. Bouchiat, and J. C. Cuevas, *Phys. Rev. B* **77**, 165408 (2008).